

# Brain Metabolic Network for the Early Diagnosis of Mild Cognitive Impairment Based on 18F-FDG PET

Pinmei Wang, Weiming Zeng

Digital Imaging and Intelligent Computing Laboratory, School of Information Engineering,  
Shanghai Maritime University, Shanghai 201306

## Abstract

**Background:** Mild cognitive impairment (MCI) is the prodromal stage of Alzheimer's disease (AD), which is divided into early MCI (eMCI) and late MCI (lMCI). Distinct from classifying AD from normal control (NC) group, there are few investigations about classifying eMCI from NC. Also, it is more difficult for us to diagnose MCI, especially eMCI due to that the clinical symptoms of MCI are slight, and the structural and functional change of the brain of eMCI is of subtle different from those of NC. On the other hand, the computer-aided early diagnosis of MCI and eMCI is of great significance to the early intervention of AD. Meanwhile, many researches showed that there are great differences between AD and NC in the structure and function of the brain network. This research therefore aimed to conduct early diagnosis of MCI based on brain metabolic network and to explore the metabolic and topological difference between eMCI, MCI and NC. **Methods:** 18F-fluorodeoxy-glucose positron emission tomography (18F-FDG PET) were collected in a cohort of individuals, including 53 with eMCI, 59 MCI and 59 NCs, and a brain metabolic network was constructed for each subject. We further divided the brain networks into two networks -- positive and negative networks according to the positive and negative connections between nodes. And then we extracted metabolism related features and topological features of the positive and negative networks. After twice feature selection, we selected the optimal features and input it into SVM for classification. **Results:** In this experiment, 88.9 percent and 88.39 percent accuracy were reached using metabolism-related features for the classification of those three groups and the classification of the pair of eMCI/NCs, respectively. Compared with eMCI, some new brain regions with significant metabolic differences were observed in MCI in this experiment, such as Hippocampus, Angular, Amygdala, et al. And we found that the average clustering coefficient and shortest path length of eMCI and MCI are showing opposite change tendency in positive and negative networks. **Conclusions:** The research results proved that our approach based on cube-based metabolic network can be used for eMCI and MCI early diagnosis. And there are extensive differences between MCI (eMCI) and NC in the structure and function of brain network.

## Keywords

MCI, eMCI, 18F-FDG PET, brain network, SVM, SVM-RFE.

## 1. Introduction

The first case of AD was discovered by the German psychiatrist Alois Alzheimer in 1906. Later, it was named Alzheimer's disease in the 8th edition of Psychiatric Handbook published by his tutor Kraepelin. AD is a progressive neurodegenerative disease characterized by memory loss, behavior and language disorder, cognitive function decline, executive function disorder and personality changes [1-3], whose etiology has not been determined yet. AD affects hundreds of millions of people all over the world. According to statistics, one AD case is conformed every

three seconds in the world. And it is estimated that the number of AD patients will increase to 300 million by 2050[4-5].

MCI is the prodromal stage of AD [6,22], which is further divided into eMCI and lMCI. Currently [7-8]. As there is no effective treatment for AD [5,11], the early diagnosis and intervention for AD is of great importance to prevent or delay transformation toward AD [7-9]. Distinct from classifying AD and NC, there are few investigations about classifying eMCI from NC. Also, it is more difficult for us to diagnose MCI, especially eMCI due to that the clinical symptoms of MCI are slight, and the structural and functional change of brain of eMCI is of subtle change from those of the NC group. At present, the clinical assessment of AD is mainly based on some assessment scales, such as CDR, etc. [9]. However, these methods are often influenced by people's subjective factors. Thus, how to diagnose MCI objectively and early has become an urgent medical and social problem.

$^{18}\text{F}$ -FDG PET technique is widely used in many kinds of disease diagnosis and differential diagnosis, judgment of state of illness, evaluation of curative effect, organ function research, etc. on account of its advantages of high sensitivity, high specificity, good security and so on, is an excellent tool for early and differential diagnosis of dementia [10,12]. Glucose is the most important energy source of brain metabolism. Positron nuclide  $^{18}\text{F}$ , which can be detected and imaged by PET and be marked on glucose, thus,  $^{18}\text{F}$ -FDG PET can accurately reflect the level of glucose metabolism in organs/tissues in vivo using  $^{18}\text{F}$ -FDG as the imaging agent.

Researches of brain radiomics have showed the brain structure and function of AD patients are significantly abnormal compared with those of normal people [12-14]. Also, many studies reported that AD is a disconnection syndrome and abnormal metabolism is one of its most important neurodegenerative indicators [19-20]. In the study of the brain network, topological abnormalities in the anatomical network of AD are also found, and the efficiency and topological properties of brain functional networks of AD are obviously different from that of NC [21], such as a decreased clustering coefficient, a longer characteristic path length, reduced long-distance connections and increased short-distance connections and so on [15,22].

At present, the research on early diagnosis of AD is mostly based on the classification of AD vs. NC, or MCI vs. NC, while the research on classification of eMCI vs. NC is very rare. EMCI is the early stage of MCI, and its diagnosis is of great importance to early intervention of AD and MCI. Thus, eMCI, MCI and NC data was collected in this experiment. Our aim is to determine whether the metabolic information extracted from cube-based brain metabolic network could be used for MCI, especially eMCI and NC computer-aided early diagnosis.

## 2. Materials and Methods

### 2.1. Imaging Data

The imaging data was downloaded from ADNI database, which is a one of the most famous AD longitudinal study and contains a large number of data from different imaging equipment, different imaging agents and different image formats and etc. We downloaded a cohort of three groups of individual  $^{18}\text{F}$ -FDG PET data. The NC group has an age between 66 and 94 years old. The eMCI group has an age between 59 and 90 years old, and the MCI is between 56 and 92 years old. The NC group has a CDR = 0. The eMCI group has a CDR = 0.5. Detailed information is show in table 1.

Table 1. Characteristics of the Participants

Group	Age	CDR
NC	66~94	0
eMCI	59~90	0.5

MCI	56~92	0.5 or 1
NC, normal control; eMCI, early mild cognitive impairment; MCI, mild cognitive impairment; CDR, Clinical Dementia Rating (0.5 - very mind; 1 - mild; 2 - moderate; 3 - severe)		

## 2.2. Image Preprocessing

In the process of data acquisition and digitization, due to various reasons, such as the mechanical noise of different acquisition equipments and instruments, the images are mixed with different levels of noise. For the convenience of subsequent experiments and to ensure the accuracy and reliability of experimental results, the image preprocessing for our obtained images is needed. For 18F-FDG PET imaging, the preprocessing usually contains three steps:

(1). Format transformation: Generally, the data format we download from ADNI is DICOM (digital imaging and communications in medicine), and we need to convert it to NIFTI (neuroimaging informatics technology initiative) format. The conversion tool from DCM to NII format used in our experiment is CaPTK, which can convert all the test data in the same folder in batches and store the results in the specified files, which is very convenient;

(2). Coregister: After the first step of format conversion, we got a .nii file for each subject. But yet, it is still inappropriate for us to use these images, because they are different in voxel size, origin, spacing and even image dimension. Therefore, we need to coregister all the data into the same space. Here, we coregistered all the PET images into MNI space using SPM12, and before this, we uniformly set the origin of PET images. After coregistration, the PET images have a dimension of (91,109,91) and a voxel size of  $2*2*2$  mm<sup>3</sup>. The results of our registration of are shown in Figure 1.

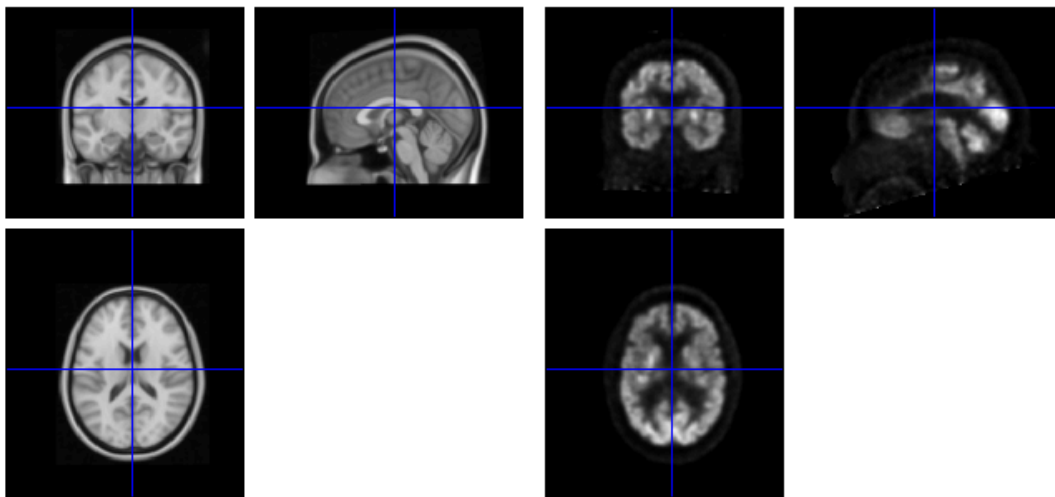


Figure 1. The results of registering PET images into MNI space using SPM12.

(3). Smoothing: Image smoothing is also an important step in image preprocessing, which can effectively suppress image noise and interference high-frequency components, make the image in gradually change and reduce abrupt gradient. Here, we use SPM12 to smooth PET images.

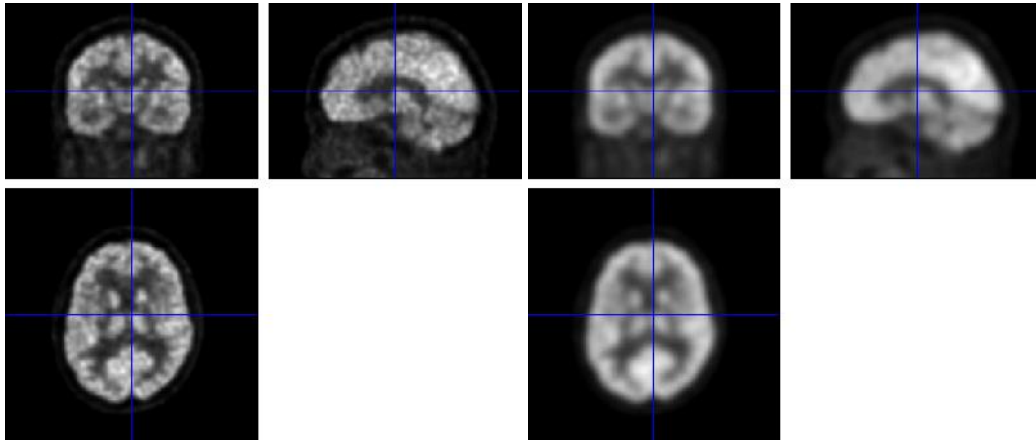


Figure 2. Smoothing of 18F-FDG PET images using SPM12

### 2.3. Brain Network Construction

After preprocessing, we constructed a brain metabolic network for each subject. In order to make a node carry enough information and reduce the computational complexity, we chose a "middle" node size for the experiment, and the node in the network is a cube with a size of  $9 \times 12 \times 9$  voxel size. Namely, we divided the whole brain into several  $9 \times 12 \times 9$  voxel-sized nodes in a non-overlapping way after selecting the seed node. The seed node we chose is the node in the upper left corner. And  $9 \times 12 \times 9$  is the size of X, Y and Z axes respectively. The edge parts with less information which are not enough to form a node was discarded. And finally, we got 900 nodes as 900 ROIs for each subjects.

We calculated the Pearson correlation coefficient between nodes as their edges, and got the correlation matrices with a size of  $900 \times 900$ . The Formula of Pearson correlation coefficient is as follows:

$$R_{XY} = \frac{\sum_{i=1}^n (V_{Xi} - \bar{V}_X) (V_{Yi} - \bar{V}_Y)}{\sqrt{\sum_{i=1}^n (V_{Yi} - \bar{V}_Y)^2} \sqrt{\sum_{i=1}^n (V_{Xi} - \bar{V}_X)^2}} \quad (1)$$

For two nodes X and Y, where n represents the number of voxels in each node, which is 972,  $\bar{V}_X$  and  $\bar{V}_Y$  represents the average value of all voxels in nodes X and Y, respectively. According Pearson correlation coefficient, we divided the network into positive and negative correlation networks, and filtered the effective edge of the network with a threshold value of  $\pm 0.3$ .

### 2.4. Feature Extraction

We extracted three kinds of features: metabolism related features and topological features of positive networks and topological features of negative networks. The metabolism related features includes mean values of all voxels in nodes and connections between nodes. The topological features contain node degree, clustering coefficient and shortest path length. In order to compare the possibility of using metabolic related features and topological features of positive and negative related networks for the early diagnosis of MCI, we conducted five experiments using those three features and their combinations respectively.

In each of the five experiments, we divided the dataset of each group of data into training set and test set in a ratio of 8:2, and carried out the corresponding features of training set to select optimal features. Then, the obtained optimal features were extracted in the test set. And finally, the SVM classification and prediction was conducted with all subjects using the optimal features.

The feature selection was conducted for the reason that the feature dimension is large, and that there are a large number of irrelevant features and redundant features in the initial extracted features, which will greatly affect the classification performance. We carried out a two-step feature selection method on the corresponding features in the five experiments to screen the distinguishing features. First of all, we use a filter method for preliminary feature selection. We

carried out the two sample t test between the three groups of subjects, and used Bonferroni correction to strictly screen features with significant differences. And we took the union of the three results as the initial feature selection results in order to keep the features that significantly distinguish the three groups of subjects. A wrapper method SVM-RFE (Support Vector Machine-Recursive Feature Elimination) was then applied for the secondary feature select to reach the final optimal features. Before using SVM-RFE, we normalized the data by min-max scaling. Data normalization scales the data with different scope into the same range, which makes the model easier to converge to the optimal solution correctly and smoothly, is a vital step to achieve good SVM performance.

## 2.5. Classification by SVM

The kernel-based SVM classification model was used in this study to predict which class a data belongs to. Similarly, we normalized the data by min-max normalization before classification. We used 10-fold cross-validation to verify our classifier. The classifier used in our experiment is fitcecoc, which is an error-correcting output codes model (ECOC) that transforms multi-classification problems into a series of two-classification problems. By default, it uses a one-by-one scheme to carry out binary classification. We also conducted the hyperparameters optimization by an 'auto' selection. The kernel used in fitcecoc is 'rbf' kernel.

## 3. Results

### 3.1. Classification Performance Based on Brain Metabolic Network

In order to compare the effects of the metabolism related features, topological features of positive and negative networks and their combinations on the early diagnosis of MCI, we calculated the average classification accuracy of the 10-fold cross-validation of different feature and their combinations. In addition, we also calculated the evaluation criteria such as sensitivity, specificity and F1 score of different groups to judge the performance of the classifier. The results are shown in Table 2.

Table 2. Classification Performance of different features and their combinations extracted from cube-based brain networks

Features	Total accuracy of three groups(%)	Groups	Accuracy (%)	Specificity(%)	Sensitivity(%)	F1 score (%)
(1)	88.9% (152/171)	NC/eMCI	88.39	88.14	88.68	91.49
		eMCI/MCI	89.29	88.68	89.83	96.36
(2)	80.1% (137/171)	NC/eMCI	80.36	80.05	77.34	88.17
		eMCI/MCI	78.57	77.36	79.66	93.07
(3)	79.5% (136/171)	NC/eMCI	75.89	79.66	71.70	81.72
		eMCI/MCI	79.46	71.70	86.44	93.58
(4)	88.3% (151/171)	NC/eMCI	84.82	84.75	84.91	90.00
		eMCI/MCI	90.18	84.91	94.92	96.55

(5)	86.0% (147/171)	NC/eMCI	83.93	86.44	81.13	88.66
		eMCI/MCI	85.71	81.13	89.83	94.64

(1). Metabolism related features (mean value of all voxels in a node + connections between nodes); (2). Topological features of positive network; (3). Topological features of negative network; (4). Metabolism related features + Topological features of positive network; (5). Metabolism related features + Topological features of negative network;

Although the features and the number of features used for SVM training are different, we can see from the table that the effect of metabolism related features is generally higher in the total classification results. The accuracy reached 88.39% and 89.29% in distinguishing the patients with eMCI from NC subjects and patients with MCI, respectively. And also, its ability to distinguish positive cases from negative cases is balanced from aspects of specificity and sensitivity. By contrast, whether it is a positive or a negative correlation network, the classification accuracy of the optimal features obtained by selecting features only from the topological features of them is generally low, and its classification effects on positive and negative cases are quite different. However, the network's topological features combined with the metabolism related features have improved its classification effect, but its ability to distinguish positive and negative cases is still not well-balanced.

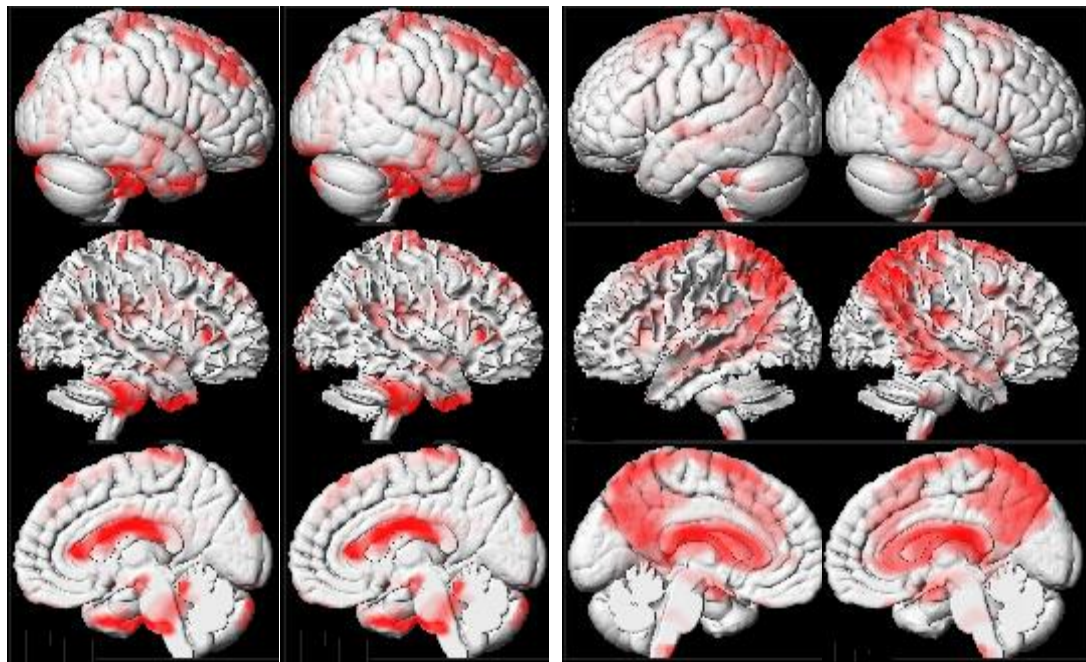
A list of the comparison of the accuracy of distinguishing eMCI from NC between other experiments and ours was made.

Table 3. Classification comparison between some previous studies and ours in distinguishing eMCI from NC

Methods	Data	Accuracy (%)
Ninon et al.[17]	18F-FDG PET (68EMCI,89NC)	64.0
Forouzannezhad P et al.[10]	MRI+PET (296EMCI, 248 NC)	78.8
Fang C et al.[9]	MRI+PET (297 EMCI, 251 NC)	79.25
Forouzannezhad P et al.[7]	MRI+PET (296EMCI, 248 NC)	84.0
Biao J et al.[18]	rs-fMRI (50EMCI, 48NC)	84.6
ours	18F-FDG PET (53EMCI,59NC)	88.39

### 3.2. Metabolic Differences

We carried out two sample t test using SPM12 and compared the metabolic differences in voxel level between different groups. Taking eMCI vs. NC and MCI vs. NC as examples, the results are shown in the figure 3.



(B)

Figure 3. (A) Metabolic difference between eMCI and NC groups using two sample t test (p-value = 0.01, cluster size > 100). (B) Metabolic difference between MCI and NC groups using two sample t test (p-value = 0.1, cluster size > 100).

As shown in Table 4 and Table 5, we listed the brain regions where the clusters with significant metabolic differences are located.

Table 4. Brain regions with significant metabolic difference between eMCI and NC

MNI coordinate	Cluster location (AAL template)	Brodmann area	Cluster size
-10 10 22	Temporal_Mid, Temporal_Pole_Sup_L, Occipital_Sup_L, Occipital_Mid, Temporal_Sup_L, Fusiform_R, Cuneus, Parietal_Lob_Inf, parahippocampa, Postcentral, Uncus, Insula_L, Anterior cingulate, Parietal_Inf, Caudate	37, 42, 22, 19, 21, 18, 38	32103
34 -4 -16	Frontal_Inf_Orb_R, Temporal_Sup, Amygdala_R, parahippocampa	13, 47	399
-32 36 46	Precentral, Frontal_Sup_Medial, Frontal_Inf	8, 9, 6, 10, 46	3076
38 46 34	Precentral, Postcentral, Paracentral_Lob_R, Frontal_Medial	6, 8, 9, 4	2287
44 -62 54	Parietal_Inf	40	111
p-value = 0.01, cluster size > 100			

Table 5. Brain regions with significant metabolic difference between MCI and NC

MNI coordinate	Cluster location (AAL template)	Brodmann area	Cluster size
----------------	---------------------------------	---------------	--------------

-10 4 22	Precuneus, Temporal, Caudate, Thalamus, Parietal_Inf_R, Parahippocampa, Hippocampus, Angular, Parietal_Sup, Postcentral, Frontal, Amygdala, Cingulate, Occipital_Sup_R, Uncus,	7, 40, 31	12001
58 -40 -14	Temporal_Mid_R, Temporal_Inf_R	21, 22	201
-12 8 68	Frontal_Sup_L, Frontal_Sup_Medial_L, Limbic, Cingulate, Supp_Motor_Area_R, Frontal_Mid	6	612
-46 -58 50	Parietal_Inf_L, Angular_L	40, 7	408
-20 -76 52	Precuneus, Parietal_Sup	7	184
-28 -42 72	Postcentral, Parietal_Sup_L	5	304
42 -32 66	Parietal	-	107
p-value = 0.1, cluster size > 100			

In our results, brain regions with significant metabolic difference between eMCI and NC are mainly located in Temporal, Occipital, Fusiform\_R, Cuneus, parahippocampa, Anterior cingulate, Insula\_L, Parietal\_Lob\_Inf, etc. And those between MCI and NC are mainly resided in Precuneus, Temporal, Thalamus, Caudate, Parietal\_Inf\_R, Frontal, Hippocampus, Angular, Occipital\_Sup\_R, Amygdala, etc. We found that these brain regions with significant metabolic differences are mainly concentrated in the association cortices regions, such as that the Temporal lobe is an important area of human memory, which is also related to hearing and language comprehension. We also found that these areas are related to the default mode network (DMN), such as the hippocampus involved in forming new memories and remembering the past, the Angular connecting perception, attention, spatial cognition and action, and the Precuneus involving vision, sensory movement and attention information, which were metabolically abnormal in both the eMCI and MCI groups. Abnormalities in glucose metabolism usually suggests abnormal brain function and neural activity, is one of the most vital indicators of neurodegeneration in AD [19].

### 3.3. Clustering Coefficient and Shortest Path Length

Topological attributes are an important feature of brain networks. Many previous studies have reported that the topological structure of metabolic brain networks in AD is different from that of normal people. We calculated the difference between three groups of the average clustering coefficient and shortest path length with a sparsity of 25-50% 500 times, as shown in Figure 4 and Figure 5.

We found that in the positive and negative correlation networks, the overall level of NC group is higher than that of EMCI group and MCI group in both clustering coefficient and shortest path length. But in between eMCI and MCI, the clustering coefficient and shortest path length are showing opposite tendency of change in positive and negative correlation network, which may explain the difference in function and effect between them: the compensation mechanism of negative correlation network.

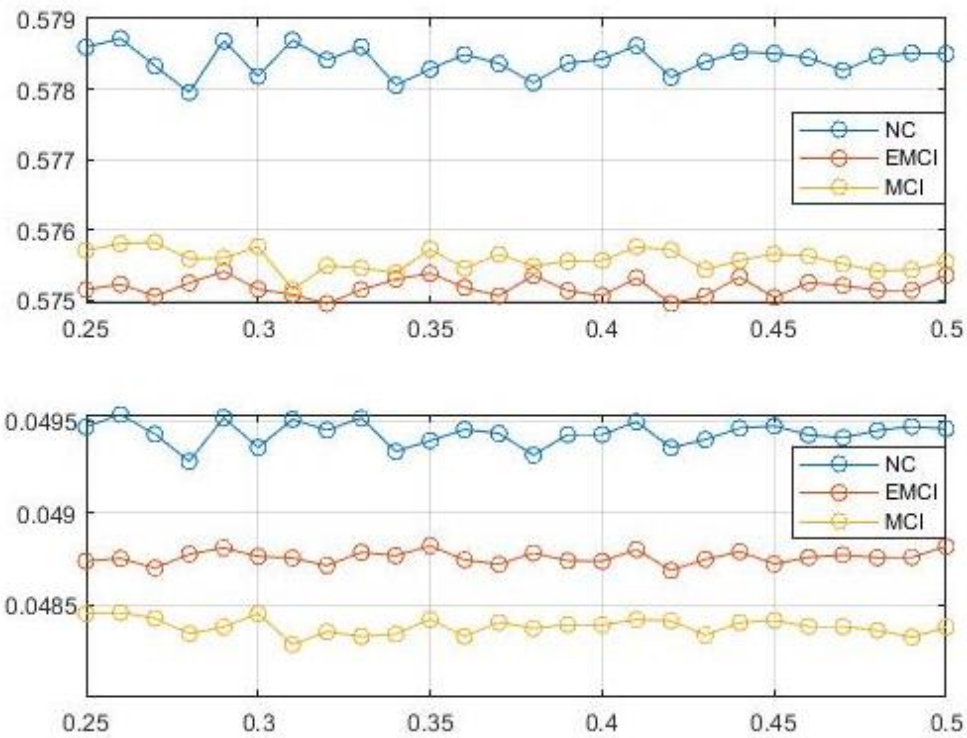


Figure 4. Average clustering coefficient and shortest path length of three groups in positive correlation network under a sparsity of 25%~50% for 500 times. (Upper: clustering coefficient, Down: shortest path length).

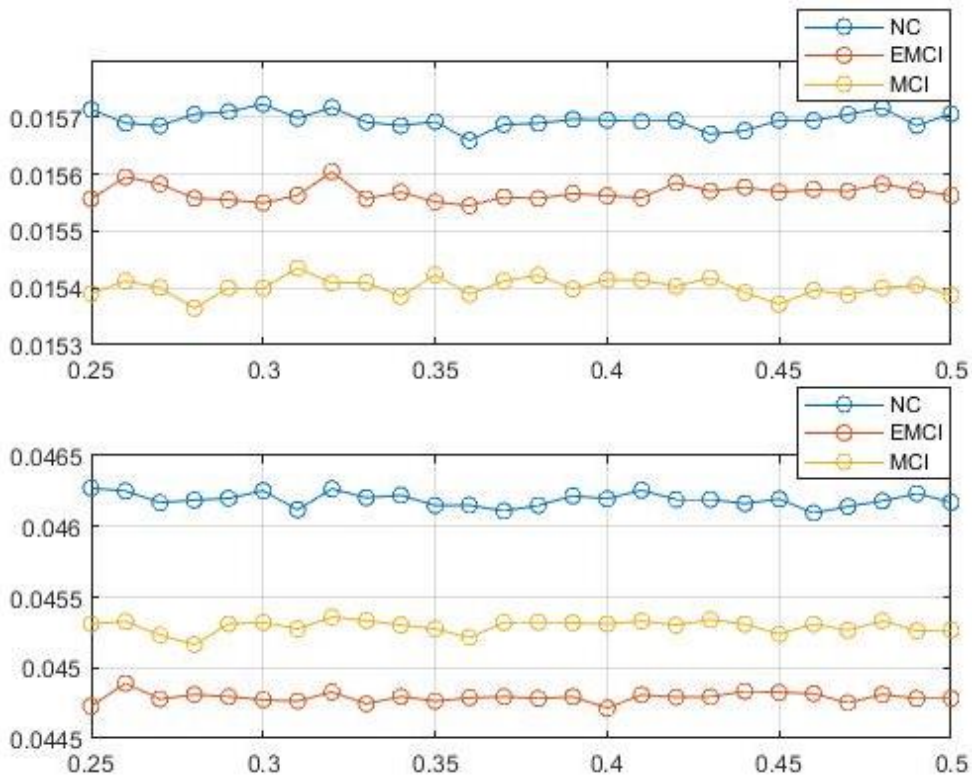


Figure 5. Average clustering coefficient and shortest path length of three groups in negative correlation network under a sparsity of 25%~50% for 500 times. (Upper: clustering coefficient, Down: shortest path length).

## 4. Discussion

Compared with traditional AD early diagnosis methods based on AD vs. NC or MCI vs. NC, this paper studies MCI early diagnosis based on MCI, eMCI and NC data. And in contrast with previous studies of directly taking brain regions or voxels as ROIs, this paper uses a structure between brain regions and voxels, cubes as our ROIs. At the same time, this study divides brain networks into positive and negative correlation networks and investigated the possibilities of their topological attributes as the biomarker of MCI early diagnosis.

The reason why our study uses fewer samples but obtains better classification accuracy is as follows: (1). Appropriate size of ROI: The ROI size is proper, so that it could bring more effective and distinguishing features, which lead to the good performance of classification. (2). Two-step feature selection: The combination of filter and wrapper method brings advantages like maximizing correlation and minimizing redundancy.

However, there is also some shortcomings in our experiments, such as that we have not further explore our classifier performance on larger samples, we also did not consider different methods, such as different feature selection methods, different classification model may influence the result of the experiment. At the same time, distinct from the voxel or brain regions, the physiology significance of the constructed cube is not strict, while it does provide more information than the brain regions, it greatly reduces the amount of computation we have to do relative to voxels.

## References

- [1] Kim J, Lee B. Identification of Alzheimer's disease and mild cognitive impairment using multimodal sparse hierarchical extreme learning machine[J]. *Human Brain Mapping*, 2018.
- [2] Aidos H, Duarte J, Fred A, et al. Identifying regions of interest for discriminating Alzheimer's disease from mild cognitive impairment. 2014 IEEE International Conference on Image Processing (ICIP), Paris, France, 2014, pp. 21-25.
- [3] Lu D, Popuri K, Ding G W, et al. Multiscale Deep Neural Networks based analysis of FDG-PET images for the Early Diagnosis of Alzheimer's Disease[J]. *Medical Image Analysis*, 2018: S13618-41518300276.
- [4] Li Y, Jiang J, Lu J, et al. Radiomics: A novel feature extraction method for brain neuron degeneration disease using 18F-FDG PET imaging and its implementation for Alzheimer's disease and mild cognitive impairment[J]. *Therapeutic Advances in Neurological Disorders*, 2019, 12.
- [5] Liu M, Cheng D, Yan W. Classification of Alzheimer's Disease by Combination of Convolutional and Recurrent Neural Networks Using FDG-PET Images[J]. *Frontiers in Neuroinformatics*, 2018, 12:35-.
- [6] Yao Z, Hu B, Nan H, et al. Individual metabolic network for the accurate detection of Alzheimer's disease based on FDG-PET imaging[C]. *IEEE International Conference on Bioinformatics & Biomedicine*. IEEE, 2017.
- [7] Forouzaneshad P, Abbaspour A, Li C, et al. A Deep Neural Network Approach for Early Diagnosis of Mild Cognitive Impairment Using Multiple Features[C]. 2018 17th IEEE International Conference on Machine Learning and Applications (ICMLA). IEEE, 2018.
- [8] Jiang J, Kang L, Huang J, et al. Deep Learning based Mild Cognitive Impairment Diagnosis Using Structure MR Images[J]. *Neuroscience Letters*, 2020, 730:134971.
- [9] Fang C, Li C, Forouzaneshad P, et al. Gaussian Discriminative Component Analysis for Early Detection of Alzheimer's Disease: A Supervised Dimensionality Reduction Algorithm[J]. *Journal of Neuroscience Methods*, 2020, 344:108856.
- [10] Forouzaneshad P, Abbaspour A, Li C, et al. A Gaussian-based model for early detection of mild cognitive impairment using multimodal neuroimaging[J]. *Journal of Neuroscience Methods*, 2019, 333:108544.
- [11] Titov D, Diehlschmid J, Shi K, et al. Metabolic connectivity for differential diagnosis of dementing disorders[J]. *Journal of Cerebral Blood Flow & Metabolism*, 2017, 37(1):252.
- [12] Kie A, Yuhei C, Saki H, et al. Influence of plasma cytokine levels on the conversion risk from MCI to

- dementia in the Alzheimer's disease neuroimaging initiative database[J]. *Journal of the Neurological Sciences*, 2020, 414:116829.
- [13] Lin S Y, Lin C P, Hsieh T J, et al. Multiparametric graph theoretical analysis reveals altered structural and functional network topology in Alzheimer's disease[J]. *NeuroImage: Clinical*, 2019, 22.
- [14] Hett K, Ta V T, JV Manjón, et al. Multi-scale Graph-based Grading for Alzheimer's Disease Prediction[J]. 2019.
- [15] Liu Y, Yu C, Zhang X, et al. Impaired Long Distance Functional Connectivity and Weighted Network Architecture in Alzheimer's Disease[J]. 2014.
- [16] Zhengjia D, Qixiang L, et al. Disrupted structural and functional brain networks in Alzheimer's disease[J]. *Neurobiology of Aging*, 2018, 75:71-82.
- [17] Ninon, Burgos, Jorge, et al. Early Diagnosis of Alzheimer's Disease Using Subject-Specific Models of FDG-PET Data[J]. *Alzheimer's & Dementia*, 2017.
- [18] Biao, Jie, Mingxia, et al. Developing Novel Weighted Correlation Kernels for Convolutional Neural Networks to Extract Hierarchical Functional Connectivities from fMRI for Disease Diagnosis[J]. *Machine learning in medical imaging. MLMI (Workshop)*, 2018, 11046:1-9.
- [19] Sun X, Nie B, Zhao S, et al. Distinct relationships of amyloid-beta and tau deposition to cerebral glucose metabolic networks in Alzheimer's disease[J]. *Neuroscience Letters*, 2019, 717:134699.
- [20] Ba Loni P, Funk C C, Yan J, et al. Metabolic Network Analysis Reveals Altered Bile Acid Synthesis and Cholesterol Metabolism in Alzheimer's Disease[J]. *Social Science Electronic Publishing*, 2020.
- [21] Chen J, Liu C, Peng C K, et al. Topological reorganization of EEG functional network is associated with the severity and cognitive impairment in Alzheimer's disease[J]. *PHYSICA A-STATISTICAL MECHANICS AND ITS APPLICATIONS*, 2018: S0378437118311609-.
- [22] Liu J, Pan Y, Wu F X, et al. Enhancing the feature representation of multi-modal MRI data by combining multi-view information for MCI classification[J]. *Neurocomputing*, 2020, 400.